Journal of Inorganic and Organometallic Polymers and Materials (2023) 33:1306–1316
https://doi.org/10.1007/s10904-023-02562-7

RESEARCH

Recycled Polypropylene Waste as Abundant Source for Antimicrobial, Superhydrophobic and Electroconductive Nonwoven Fabrics Comprising Polyaniline/Silver Nanoparticles

Ayman Nafady[1] · Munirah D. Albaqami[1] · Amerah M. Alotaibi[1]

Received: 14 December 2022 / Accepted: 26 January 2023 / Published online: 4 March 2023

Abstract
Recently, studies focusing on the development of multipurpose nonwoven polypropylene fabric have attracted a great attention owing to their widespread applications. Herein, we pad-dry-cured silver nitrate and aniline monomer into plasma-pretreated nonwoven polypropylene fabrics to in situ create a nanocomposite film comprising both silver nanoparticles (AgNPs) and polyaniline to introduce multifunctional properties. In doing so, nonwoven fibrous mat was initially fabricated by subjecting shredded recycled polypropylene waste to melt-spinning. Polyaniline was then produced on the fabric surface via a redox polymerization of aniline, which caused concomitant reduction of Ag^{+} ions into Ag^{0} as nanoparticles. In this composite, AgNPs served as an antimicrobial agent whereas polyaniline worked as an electrical conductor. Importantly, superhydrophobic characteristics were imparted to polypropylene textiles by microwave-assisted curing with trimethoxyhexadecylsilane. Scanning electron microscopy, transmission electron microscopy, energy-dispersive X-ray spectroscopy, and Fourier-transform infrared spectroscopy have been utilized for morphological analyses. To determine the level of comfort provided by the final nonwoven polypropylene products, their stiffness and breathability were explored. The antimicrobial effectiveness of the AgNPs-treated fabrics against *S. aureus* and *E. coli* was evaluated. Finally, the prepared polypropylene fabrics demonstrated high blocking to UV rays along with superior electrical conductivity, making these fabrics promising for medical applications such as wound treatment, protective coatings and wearable electronics.

Keywords Plasma activation · Microwave heating · Polyaniline · Silver nanoparticles · Multifunctional nonwoven polypropylene

1 Introduction

Textiles fabrics are highly valuable owing to their softness, lightweight, flexibility, strength, gas and gas penetration along with their desirable physico-mechanical features that make attractive candidates in sensors, heat and radiation shields, electronic displays, air and water filtration systems, and medical field [1–5]. In this context, wearable smart textile sensors can track and adjust parameters like temperature and muscle vibration during physical activity while therapeutic substances can be slowly released into human skin [6–8]. Other related applications of smart clothing include bio-monitoring, wearable wireless communications, public telecontrol and telemedicine [9–11]. Success in creating highly efficient electrically conductive materials, especially for use in healthcare, has been a significant research endeavor. Therefore, it is possible to build a "bionic human" with the use of electrically conductive textile materials to replace metal-based dysfunctional muscles. This might allow a person with a disability to shop independently [12–14].

Among the methods used to manufacture electrically conductive textiles are coating fibers with electroconductive metallic layer, embedding metallic wires into yarns, or inclusion of conductive fillers [15, 16]. Unfortunately, not enough research has been undertaken into immobilizing conductive polymers into smart multifunctional textiles [17]. Conjugated electroconductive polymers, such as polyaniline, polythiophene, and polypyrrole have recently been introduced into conductive fibers, with polyaniline (PANi)

✉ Ayman Nafady
anafady@ksu.edu.sa

[1] Department of Chemistry, College of Science, King Saud University, 11451 Riyadh, Saudi Arabia

being the most essential conductive polymers [18, 19]. As a result, PANi has been used in a wide variety of technologies, including actuators, chemical and electrochemical sensors [20–22], batteries and supercapacitors, solar cells, electrochromic smart windows, flexible transparent displays, electronic circuits, and electroluminescent devices [19]. The importance of electron spin in the electrical conductivity of conductive polymers, particularly in PANi, has been recently studied [23].

Polymer-based electronics and military gadgets have shown widespread application in a range of settings, but there is concern that they may generate hazardous amount of electromagnetic interference that might damage other devices and people [24]. Since then, several magnetically and electrically conductive materials have been investigated as microwave absorbers and electromagnetic interference armors, such as metallic nanoparticles and conducting polymers [25, 26]. The effectiveness of electromagnetic interference shielding is highly dependent on the filler properties like its composition, dielectric constant, dispersion, thickness, and percentage. Owing to the unique properties of silver nanoparticles (AgNPs) such as strong antibacterial activity, resistance to UV radiation, and capacity to self-clean by a photocatalytic process [27–29], microwave-absorbing composites can be created by using AgNPs as a filler in polymer media.

Improvements in binding of colloidal nanoparticles to polypropylene fabrics were accomplished after plasma curing of the fiber surface [30, 31]. Oxidative-creation of grooves and engravings during the plasma curing process has been found to cause the formation of oxygen-containing polar groups on the polypropylene surface. These groups, which include hydroxyl, carboxyl, and ester groups, increase the binding of nanoparticles to fibers. When it comes to modifying the surface topmost atomic layer without impacting the bulk characteristics, plasma techniques have been regarded as a sustainable option [32]. In situ synthesis of PANi into synthetic textile fibers has been described using a variety of methods such as electrochemical, block, and graft polymerization [33]. The in situ integration of AgNPs/PANi composite into polypropylene has not been extensively investigated despite being significant to develop multifunctional polypropylene fibers. Thus, high technologies are required to make the concept of simple wearable interfaces between gadgets and customers, providing people access to healthcare, help, and data. Multipurpose "smart" clothing has the potential to enhance human well-being in numerous important ways, including health and security. For its low cost and strong mechanical properties [34–36], polypropylene has quickly become one of the most widely used fibers. Polypropylene fabrics have exceptional durability and are resistant to a wide range of chemicals, dampness, and electricity. Historically, polypropylene textiles have played an important role in several industries, including food and beverage, medical device, and automobile industries. However, polypropylene textiles are stain-resistant as they lack active coloring sites. To improve the polypropylene coloration properties and binding to different helpful agents like PANi and AgNPs [37, 38], plasma curing has been reported as an ecologically friendly process.

In this contribution, we describe facile development of a new multifunctional nonwoven polypropylene fabric that will provide UV protection, antimicrobial characteristics, electrical conductivity, along with superb water repellency. Polypropylene waste was firstly shredded and put through a melt-spinning process to provide nonwoven fibrous mat. During the pad dry curing process at room temperature, the polypropylene fibers absorb the water-soluble aniline monomer and silver ions. To make AgNPs, we benefited from the oxidative potential of silver nitrate ($AgNO_3$) dissolved in water by adding an electrically conductive polyaniline as a reducing agent. Hydrophobic materials have been developed for a variety of applications such as protective textiles, oil/water separation, oil resistance, self-cleaning performance, and maritime industries [1, 39–43]. A material can be described as superhydrophobic when its surface has a static water contact angle higher than 150°, and a sliding angle less 10° [44–46]. Trimethoxyhexadecylsilane (TMHDS) has been employed to develop superhydrophobic surfaces. TMHDS was immobilized onto polypropylene under microwave heating that presents an efficient heating method [47] as compared to conventional heating because it is characterized by lower cost, faster processing, uniformity of heating, lower energy consumption, and accurate temperature control [48–51]. The treated fabrics were examined using SEM, FT-IR, TEM, and EDX. Based on experimental evidence, polyaniline was synthesized alongside AgNPs that developed uniform layer over polypropylene fibrous surface. High deposition density and homogeneous dispersion of PANi and AgNPs in the nano-structured thin film were observed, indicating a particle size of 5–18 nm. In order to evaluate the superhydrophobic performance of the AgNPs/PANi-finished textiles, the contact angle was measured. Cured fabrics' comfort characteristics are unaffected by the oxidation-reduction polymerization process. Importantly, the colorfastness of the nonwoven polypropylene textiles was persistent against washing, perspiration, rubbing, and light. This easy, harmless to environment and inexpensive method might be of potential use in the creation of new multifunctional polypropylene textiles, such as medical apparel.

2 Experimental

2.1 Reagents and Materials

Trimethoxyhexadecylsilane (TMHDS), ammonium acetate (CH_3COONH_4), silver nitrate ($AgNO_3$), and aniline were

purchased from Aldrich and used as received. Recycled polypropylene chips were dried at 140 °C before being extruded for use in melt-spinning. The mechanical needle punching method was utilized to manufacture the nonwoven polypropylene textiles [52].

2.2 Plasma System

As shown in Fig. 1, two Cu-electrodes (2.5 cm in diameter) were placed in parallel in the device. These electrodes had a separation of 1.1 mm between them. The Cu-electrode was made porous by coating it with sheets of Al_2O_3 (4 cm in diameter and 3.5 mm in thickness) [53]. A high voltage convertor provided the power, which was delivered in a sinusoidal wave at 50 Hz. Atmospheric pressure was used for the discharge's open system. Oscilloscope (40 MHz) readings of the functional potential (Va). By taking a reading of the voltage across the resistance ($R_1 = 100$), the current was calculated. The voltage between the electric plates was determined using a potential separator of resistance ($R_2/R_3 = 500$).

2.3 Plasma Treatment

A glow discharge low-pressure/low-temperature plasma device (13.56 MHz) was utilized to cure the nonwoven polypropylene fabric. Oxygen plasma is used as the gas source to treat the nonwoven polypropylene textile. The nonwoven polypropylene (10×15 cm) was positioned at the reactor centre, between two electrodes. The cloth was treated with plasma for 5 min at 400 W of power and 200 cm^3/min of gas flow at standard atmospheric pressure (3×10^3 mbar). Negative charges on the nonwoven polypropylene fabric resulted from the introduction of oxygen-containing substituents. The production of atomic and ionized oxygen led to the formation of those oxygen-containing substituents.

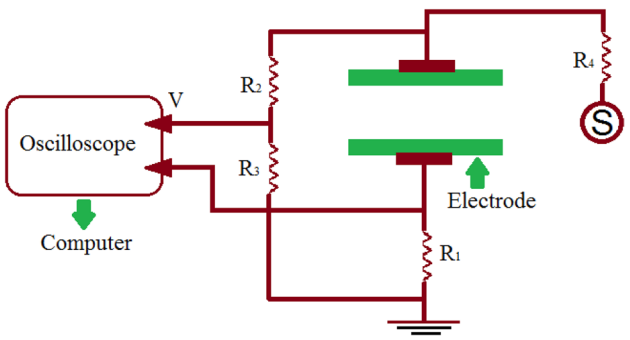

Fig. 1 Description of plasma set-up

2.4 Preparation of Multifunctional Polypropylene

To in situ embed the water-insoluble AgNPs/PANi particles into the polypropylene fabric, the textile substrates that had been plasma-cured were soaked in an aqueous mixture of aniline (10 g/L), CH_3COONH_4 (20 g/L), and $AgNO_3$ (100 ppm) at 30 °C for 30 min at a liquor ratio of 1:50. The polypropylene substrates were rinsed in water and air dried. To prepare a PANi-loaded fabric, plasma-treated cloth (liquor ratio 50:1) was soaked in aniline (10 g/L) and CH_3COONH_4 (20 g/L) at 30 °C for 30 min at a liquor ratio of 1:50. Superhydrophobic nonwoven fabrics were made by treating polypropylenes with TMHDS (3%; v/v) in an ethanolic solution for 1 h at room temperature, and drying them at 75 °C for five minutes. The fabrics were then exposed to microwave irradiation for 180 s at a power of 90 W using KOG134K MW Oven (1000 W). Plasma-untreated (PP_1) and plasma-treated (PP_p) nonwoven polypropylene fibers, PANi-finished plasma-uncured (PP_2) and plasma-cured (PP_3) polypropylene fibers, AgNPs/PANi-finished plasma-unetreated (PP_4) and plasma-pretreated (PP_5) polypropylene fibers, and AgNPs/PANi/TMHDS-finished plasma-uncured (PP_6) and plasma-cured (PP_7) polypropylene samples were all provided herein.

2.5 Methods and Apparatus

The morphologies of nonwoven polypropylene samples were studied with a Quanta FEG250 scanning electron microscope (Czech Republic) at 30 kV, whereas their elemental composition was analyzed using an EDX analyzer (TEAM-EDX) linked to SEM at acceleration voltages of 20 kV and 1 nA. The average particle size was measured using Image J program. JEOL 1230 TEM (Japan) was used to study the morphology of silver nanoparticles. After the reaction system of PP_5 (plasma-pretreated AgNPs/PANi-immobilized polypropylene fabric) changed color from transparent to dark brown, a sample of Ag^0 nanoparticles was isolated for TEM analysis. FTIR spectra (transmittance; 400–4000 cm^{-1}) were collected using a Nexus 670 (Nicolet; USA) as the nonwoven polypropylene was in contact with the detector. The contact and sliding angles of the nonwoven polypropylene textiles were measured using a Dataphysics OCA15EC (Germany). The gas permeability was examined using Textest FX3300 and ASTM D737 standard test method [54]. A total of three readings were collected from various points on the fabric, and the results were averaged. Nonwoven polypropylene stiffness was measured using a Shirley stiffness machine as specified by the British 3356:1961 standard method. The electrical conductivity of the nonwoven polypropylenes was measured using HIOKI LCR Hi 3522-50 (Japan) [55]. Electrical conductivity was measured three times and averaged. Evaluation of UV-shielding was carried out by measuring

UV-Vis transmittance spectra from 280 to 400 nm (UVB and UVA) at 1 nm intervals, as per AATCC 183(2004) standard technique [56]. AATCC(100-1999), a standard method for counting microorganisms, was used to evaluate the antibacterial activity of the nonwoven polypropylene fabrics against *Escherichia coli* and *Staphylococcus aureus*. The colorimetric changes were assessed by UltraScan PRO HunterLab (USA) utilizing color intensity (*K*/*S*) and CIE Lab, where L* is lightness from black(0) to white(100), a* is the red(+a*) to green(−a*) colorimetric ratios, and b* is the yellow(+b*) to blue(–b*) colorimetric ratios [36]. ISO105 protocols were used to document the colorfastness properties, including E04(1989) for sweat, the X12(1987) for rubbing, B0(1988) for light, and the C02(1989) for washing.

3 Results and Discussion

3.1 Preparation of Technical Polypropylene Textile

The present work was motivated by the high demand to immobilize AgNPs and PANi onto nonwoven polypropylene fabrics in order to possibly generate antibacterial, superhydrophobic, and electrically conductive textiles. Synthesizing AgNPs onto polypropylene in situ by oxidative polymerization of polyaniline is an efficient way to cut down on post-production costs. Plasma-activated polypropylene fibers were made by exposing the fibers to a low-pressure plasma irradiation, which is supposed to induce the formation of negative charges onto the surface of polypropylene by forming oxygen-containing groups like –O–O– and –COO– [57]. In the course of the plasma curing procedure, atomic and ionized oxygen were produced, leading to the formation of these oxygen-rich groups. Silver nanoparticles/Polyaniline (AgBPs/PANi) was in situ incorporated onto polypropylene by padding the plasma-activated samples at room-temperature in an aqueous combination of aniline, CH_3COONH_4, and $AgNO_3$. To make PANi-finished polypropylene textiles, the plasma-cured polypropylenes were also processed using the pad-dry-curing technique in an aqueous combination of CH_3COONH_4 and aniline. To achieve the superhydrophobic effect, polypropylene fabrics imbedded with PANi or AgNPs/PANi were treated with an ethanolic solution of TMHDS by the pad-dry-cure procedure at room temperature and then cured under microwave heating. Electroconductive, superhydrophobic, and antibacterial nonwoven polypropylene were the outcomes of these processes. The redox procedure comprises a reducing process of $AgNO_3$ to AgNPs associated with oxidizing aniline to PANi, and then treating the mixture with TMHDS. Polypropylene fabric immobilized with AgNPs/PANi/TMHDS is the result of these interdependent processes [58]. Simultaneously with the in situ reduction of silver ions (Ag^+) to metallic silver (Ag^0), the oxidative polymerization of aniline to PANi took place. In Fig. 2, the redox process presented a reduction of Ag^+ and oxidative polymerization of aniline, which results in the synthesis of AgNPs and PANi. The reaction mixture changed from clear to dark brown when the water-soluble Ag^+ were converted to the water-insoluble Ag^0, which was subsequently trapped in situ inside polypropylene fibers. The color change is due to an increase in absorbance intensity at a short wavelength of visible light, which is caused by the plasmon effect. Surface plasmon resonance is a phenomenon that occurs when AgNPs interact with the electromagnetic spectrum, causing a coherent oscillation of the conductive free electrons, resulting in a significant absorption peak.

3.2 Morphological Studies

Figures 3 and 4 present the results of structural-morphology analyses performed on polypropylenes using FTIR, SEM, TEM, EDX, and elemental mapping. The immobilization of AgNPs, PANi, and TMHDS on the fabric surface was analyzed using SEM images (Fig. 3a, b). The fibrous surface of the blank polypropylene was rather smooth, in contrast to the rough surface of the AgNPs/PANi/TMHDS-finished polypropylene fibers that were treated with plasma. Indications of etching were seen on the surface of the plasma-cured fabrics. Observations of the surface of plasma-treated polypropylene revealed the presence of microscopic granules, microcraters, and ripples. Plasma curing was used to erode the top surface layer, which resulted in the formation of surface grooves and engravings that are very helpful for the strong binding of AgNPs. Fabrics that were subjected to plasma curing produced a homogeneous coating of PANi or AgNPs/PANi under redox reaction. The resulting AgNPs/PANi film showed a uniform dispersion throughout the polypropylene surface [8], in contrast to the PANi layer, which showed a moderate tendency to develop clusters. In addition, more AgNPs were found on the plasma-treated fabrics than on the plasma-inactivated ones. The increased chemical binding between polypropylene fibrous surface and AgNPs/PANi can be attributed to plasma-curing process [57, 59]. In

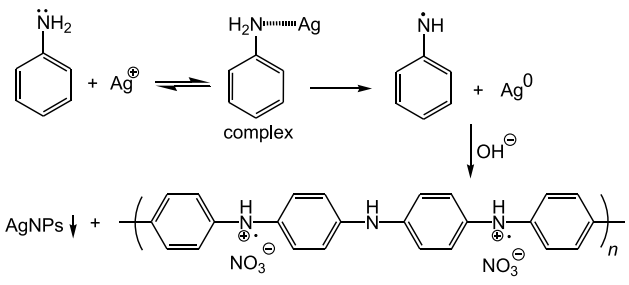

Fig. 2 Plasma-promoted redox of aniline (reducing agent) and silver nitrate (oxidizing agent) to produce PANi and AgNPs, respectively

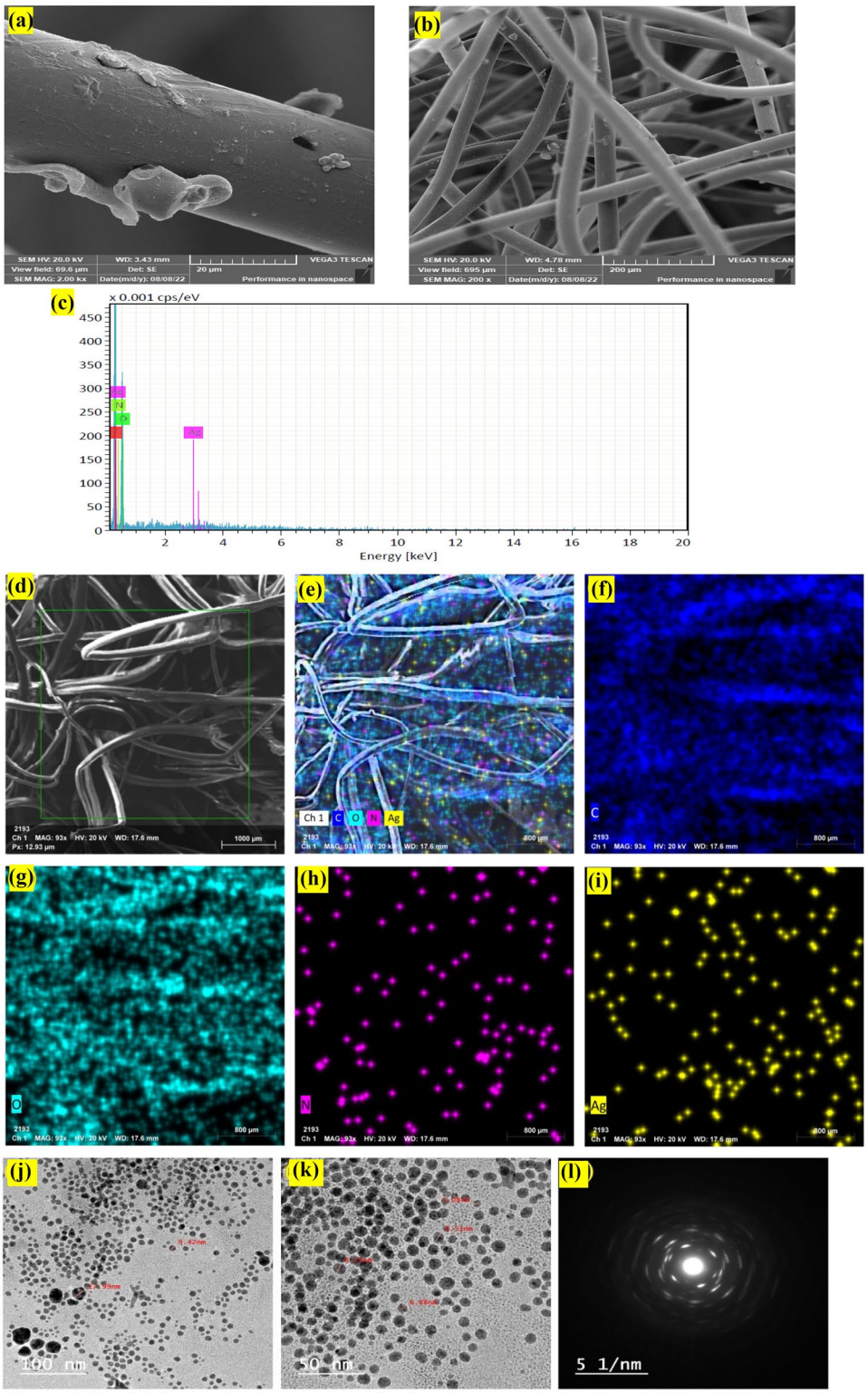

Fig. 3 **a**, **b**, **c** SEM and EDX images of AgNPs/PANi-finished plasma-treated polypropylene; a bit of fibers was taken from the fabric surface, **d** SEM image of the selected area for mapping study, **e** mapping of all elements, **f** mapping of carbon, **g** mapping of oxygen, **h** mapping of nitrogen, and **i** mapping of silver, **j**, **k** TEM images at different magnifications, and **l** selected area (electron) diffraction (c) for AgNPs

addition, crystalline micro(nano)-structures were observed in AgNPs/Polyaniline, which are preferred to improve the polypropylene conductivity. Clearly, deposited particle density has increased after TMHDS treatment. The fiber morphological properties of plasma-uncured and plasma-cured textiles were not noticeably different after TMHDS coating. The particle diameter of the treated fabrics ranged from 25 to 75 nm, as determined by particle size distribution studies performed utilizing image J software. As can be shown in Fig. 3j–l, the generated AgNPs were measured to have a

diameter of 5–18 nm using transmission electron microscopy (TEM). After the reaction system of PP_5 changed from transparent to dark brown, a sample of Ag^0 nanoparticles was extracted for TEM analysis.

The percentages of the individual elements present in the AgNPs/PANi/TMHDS-coated plasma-cured polypropylene were determined using EDX (Fig. 3c) and as listed in Table 1. The chemical compositions of the AgNPs/PANi/TMHDS film at three investigated sites were quite similar, suggesting that AgNPs/PANi/TMHDS was homogeneously dispersed over the polypropylene surface. Element mapping showed that AgNPs/PANi/TMHDS hybrid composite has been successfully adsorbed onto the plasma-activated textile surface (Fig. 3d–i). Both carbon and oxygen are assigned to the structure of polypropylene fibers, whereas silver is attributed to the structure of AgNPs. It is likely that the presence of silicon at low concentrations could be attributed to the very low TMHDS content. Successful deposition of AgNPs onto polypropylene surface was verified by the presence of Ag^0 metal as detected by EDX (Fig. 3c). Improvements in binding of colloidal silver nanoparticles to polypropylene fibers were achieved by plasma curing of the fiber surface [30]. Plasma curing was applied to erode the polypropylene surface to result in surface grooves and engravings that are very useful for the strong binding of AgNPs. The plasma-oxidative production of grooves and engravings has been known to cause the formation of oxygen-containing polar groups on polypropylene surface. These groups, which include hydroxyl, carboxyl, and ester groups, increase the binding of silver nanoparticles to fibers. Thus, the Ag ratio increases in the plasma-cured PP_7 sample compared to the plasma-uncured PP_6 sample. Oxygen levels went up while carbon dioxide dropped as a consequence of the plasma activation. This could be attributed to plasma activation which results in the formation of oxygen-containing functional groups such as hydroxyl, ester, carboxylic, and ether [57, 59]. Therefore, plasma-treated polypropylene contained higher ratio of oxygen element than untreated polypropylene. As expected, the plasma-treated fabric had lower carbon element content than the untreated fabric. It has been claimed that the FTIR spectra of both treated and untreated polypropylenes may be utilized to trace the transitions between the material's unique absorption bands. Plasma-activated polypropylenes were analyzed by Fourier transform infrared spectroscopy (FTIR), and the results are shown in Fig. 4 for blank and AgNPs/Polyaniline/TMHDS-finished polypropylene samples. The absorption peaks showed no significant deviations. The C–H (aliphatic) stretch band was detected at 2923 cm^{-1}, and the C–H (aliphatic) wagging band at 1440 cm^{-1}. The moisture was monitored at 1716 cm^{-1} due to deformation vibration of water molecules. FTIR spectral investigations of PANi, AgNPs/Polyaniline, and AgNPs/Polyaniline/TMHDS-finished plasma-cured materials did not reveal any new peaks. Thus, during the integration of PANi, AgNPs/Polyaniline, or AgNPs/Polyaniline/TMHDS, no chemical interactions took place with the polypropylene surface.

Table 1 Chemical compositions (wt%) of polypropylene fabrics

Fabric	C	O	Ag	Si	N
PP_1					
Site 1	57.65	42.35	0	0	0
Site 2	57.10	42.90	0	0	0
Site 3	57.27	42.73	0	0	0
PP_p					
Site 1	56.95	43.15	0	0	0
Site 2	56.07	43.93	0	0	0
Site 3	56.62	43.38	0	0	0
PP_6					
Site 1	57.58	41.21	0.62	0.40	0.19
Site 2	57.15	41.58	0.70	0.32	0.25
Site 3	56.62	41.75	0.81	0.52	0.28
PP_7					
Site 1	54.56	41.02	2.45	1.26	0.71
Site 2	54.99	41.00	2.24	1.02	0.55
Site 3	55.01	41.04	2.01	1.07	0.67

3.3 Ultraviolet Shielding

Protecting people from potentially dangerous ultraviolet (UV) electromagnetic radiation is a top priority; hence incorporating AgNPs as an ultraviolet shielding agent into polypropylene is essential. The test results contrasting the UPF of uncoated and coated polypropylene are shown in Table 2.

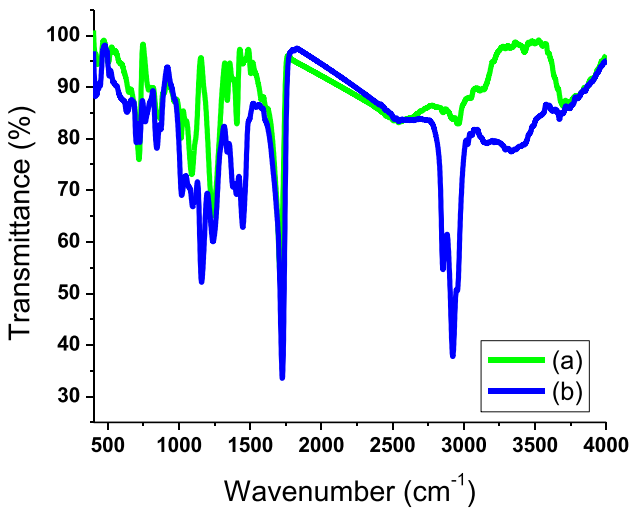

Fig. 4 FTIR spectral analysis of polypropylene textile; PP_7 (a), and PP_0 (b)

Table 2 UPF, gas-permeability, stiffness, contact angle (CA) and sliding angle (SA) of polypropylene textiles

Sample	UPF	Gas-permeability (cm^3/cm^2 s)	Stiffness (cm)		CA (°)	SA (°)
			Warp	Weft		
PP_1	98	46.64	3.5	3.7	125.0	17
PP_2	104 ± 1.1	44.06	3.9	4.1	126.2	17
PP_3	113 ± 1.0	45.76	4.0	4.2	129.8	17
PP_4	180 ± 1.5	45.51	4.1	4.4	130.9	16
PP_5	235 ± 1.5	45.10	4.1	4.4	133.0	15
PP_6	227 ± 1.3	44.68	4.3	4.5	148.4	8
PP_7	314 ± 1.6	44.03	4.4	4.6	153.6	7

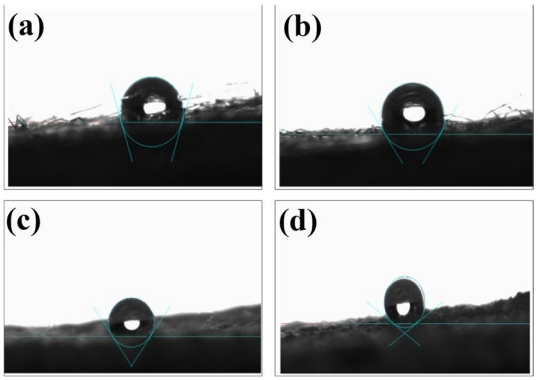

Fig. 5 Contact angles of PP_4 (**a**), PP_5 (**b**), PP_6 (**c**), and PP_7 (**d**)

PANi or AgNPs/PANi was immobilized onto polypropylene, which made the fabric more resistant to UV radiation. The plasma treatment likely increased the UPF values by attaching AgNPs to etches and engravings created on the surface of the polypropylene fibers. Since plasma curing generates negative charges of oxygen-containing groups on the fabric surface, improved Ag–O bond formation also results.

3.4 Hydrophobicity Measurements

The contact angle of plasma-uncured polypropylene was dramatically raised to 148.4° after TMHDS was inserted into the material surface (Table 2; Fig. 5). The contact angle of polypropylene textiles that had been pretreated with plasma was measured to be 153.6°, which is much higher than that of plasma-uncured AgNPs/PANi/TMHDS-finished polypropylene (contact angle: 148.4°). Plasma activation of polypropylene creates a rougher surface and a higher density of AgNPs and TMHDS, both of which may contribute to the enhanced superhydrophobic activity. As the concentration of AgNPs and TMHDS rose, so did the static contact angle. However, very high TMHDS concentrations on the polypropylene surface may substantially minimize the distance between the particles of TMHDS and AgNPs, hence reducing the surface roughness and, in turn, the contact angle [60]. Similarly, the sliding angles were found to improve upon the inclusion of TMHDS on the sample surface.

Table 3 Antibacterial assessment and electroconductivity of nonwoven polypropylene

Sample	Reduction (%)		Conductivity (S cm^{-1})
	E. coli	*S. aureus*	
PP_1	0	0	1.3×10^{-10}
PP_2	11 ± 1.1	10 ± 1.3	0.4032
PP_3	14 ± 1.1	13 ± 1.0	0.5144
PP_4	32 ± 1.0	27 ± 1.1	0.6265
PP_5	46 ± 1.6	42 ± 1.1	0.7300
PP_6	35 ± 1.0	31 ± 1.7	0.6538
PP_7	58 ± 1.5	49 ± 1.2	0.7618

3.5 Antibacterial Studies

The antibacterial investigation was done for *S. aureus* and *E. coli* employing the plate agar counting protocol, and the findings are summarized in Table 3. The blank polypropylene fabric used for the experiment showed no antibacterial activity. However, plasma pretreated/untreated samples immobilized with PANi/AgNPs/TMHDS had much better antibacterial activity than blank and PANi-immobilized polypropylene. The antibacterial activity of the plasma-treated materials was also much higher than that of the plasma-untreated polypropylene. This proves that silver nanoparticles can effectively kill many different types of bacteria. Many hypotheses have been put out to explain how AgNPs can inhibit the growth of bacteria, but the precise mechanism by which they exert their deadly effect on pathogenic germs still unknown. Larger surface area of AgNPs has been found to increase their antibacterial effectiveness. Therefore, increasing the amount of AgNPs in polypropylene might improve its antibacterial qualities. This was shown by plasma curing, which increased the affinity and binding of silver nanoparticles to the textile fibers. This means that plasma-cured textiles with a higher density of AgNPs outperform those without plasma treatment with regards to

their antibacterial efficacy. AgNPs have acquired popularity as a powerful antibacterial drug due to their ability to bind to bacterial DNA molecules and then release Ag^+ via holes in the bacterial cell wall. Therefore, Ag^+ inhibits enzyme function and kills bacteria by interacting with phosphorous in their DNA [24, 61, 62]. The effects of washing on hydrophobicity and antimicrobial activity of the treated fabrics (PP_6 and PP_7) were explored over five laundry cycles according to standard AATCC 61:1989 protocol. The durability of the treated fabrics (PP_6 and PP_7) was evaluated by recording their contact angles and antimicrobial activity after washing [63]. Both hydrophobicity and antimicrobial activity of the treated fabrics (PP_6 and PP_7) were found to relatively decrease after washing for five laundry cycles. The contact angles of PP_6 and PP_7 were reported to decrease from 148.4° and 153.6° to 144.7° and 150.3°, respectively. The reduction (%) of PP_6 and PP_7 against *E. coli* was reported to decrease from 35 to 58 to 27 and 48, respectively. Similarly, the reduction (%) of PP_6 and PP_7 against *S. aureus* was reported to decrease from 31 to 49 to 22 and 43, respectively.

3.6 Conductivity Evaluation

The findings of an examination of the electrical conductivity of polypropylene fibers loaded with PANi, AgNPs/PANi, and AgNPs/TMHDS that were either plasma treated (or plasma-untreated) are shown in Table 3. Conductivity was increased with increasing silver nanoparticles dispersed throughout a polyaniline matrix due to the synergistic effect of silver nanoparticles. The cured garments have a conductivity ranging from 0.3655 (PP_2) to 0.6860 (PP_7) S cm^{-1}. It was also found that PANi-immobilized fabric had lesser conductivity than AgNPs/PANi-coated fabric. On the other hand, the electrical conductivity of plasma-pretreated samples was enhanced compared to that of plasma-untreated textiles. A possible explanation for the increased electrical conductivity is the tighter binding of AgNPs to polypropylene surface, which reduces the distance that electrons must travel through the PANi matrix before reaching the fabric surface [64]. In order to facilitate the formation of a well-oriented polyaniline on the AgNPs surface, the AgNPs served as a suitable matrix, hence enhancing the charge transfer.

3.7 Coloration and Colorfastness

Flexibility and breathability must be maintained throughout the manufacturing of multifunctional polypropylene fibers for the treated fabric. Table 2 is a summary of gas-permeability and stiffness of treated polypropylenes. It was determined that the treatment method had no effect on either gas-permeability or stiffness in either weft or warp directions. Polypropylene textiles retain all of their physico-mechanical properties after being treated. The color information (*K*/*S* and CIE Lab values) acquired to analyze the dyeing of textiles by AgNPs is shown in Table 4. AgNPs-immobilization into plasma-inactivated polypropylene samples generated a pink color, whereas AgNPs-immobilized polypropylene samples that had been prepared with plasma showed a dark blue color (Fig. 6). Increased incorporation of AgNPs into polypropylene fibers, as evidenced by a high *K*/*S* value, allowed plasma-treated fabrics to be more effectively dyed with polypropylene than plasma-uncured polypropylene. L* was shown to dramatically decrease for both plasma-cured and plasma-uncured materials when AgNPs were generated into the surface of polypropylene, indicating a darker color. In addition, L* changed more for plasma-treated polypropylene (dark blue) than for untreated polypropylene (pink), indicating a deeper color. In general, redder colors had higher a* values, while yellower colors had higher b* values.

Table 4 Colorimetric results of polypropylene textiles

Fabric	*K*/*S*	L*	a*	b*
PP_1	0.19	92.80	0.18	1.23
PP_6	3.60	76.35	− 4.42	18.34
PP_7	6.96	64.57	− 12.01	11.85

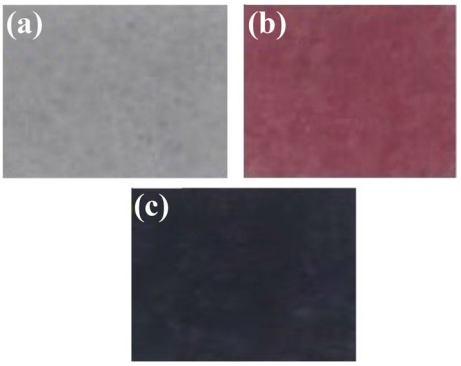

Fig. 6 Photographic images of polypropylene samples; PP_1 (**a**), PP_6 (**b**), and PP_7 (**c**) (Color figure online)

For both a* and b*, lower values suggested greener and bluer hues. Due to an increase in b* and a decrease in a*, the AgNPs-immobilized plasma-untreated polypropylene has transformed from a brighter white to a deeper pink. The dark blue hue of the AgNPs-immobilized plasma-treated polypropylene was denoted by a drop in b* and an increase in a*.

The absorbance spectra were analyzed to get insight into the chromatic activity that AgNPs provided to polypropylene fabrics (Fig. 7). In contrast to the plasma-untreated PP_4 and PP_6 (pink color), the untreated PP_5 and

PP_7 exhibited a strong absorbance band at 379 nm, suggesting a darker blue color.

Table 5 shows the ability of the treated polypropylene fabrics to resist color fading upon exposure to light, washing, sweat, and rubbing. The dyed polypropylene samples that were treated held up well against repeated washes, scrubbings, and even sweat. Significant colorfastness improvements were monitored throughout the transition from PANi-finished to AgNPs/PANi/TMHDS-finished polypropylene. Additionally, the plasma-cured samples had better colorfastness than the plasma-uncured ones. The colorfastness findings scored highest (very good to outstanding) for the AgNPs/PANi/TMHDS-finished samples that were treated with plasma. Stronger linkages were created between the AgNPs/PANi in the plasma-treated samples, which may explain why they held up better over time. Strong Ag–O bonding allowed the polypropylene fibers to more effectively stabilize the AgNPs/PANi on the fabric surface. By eliminating the need for additional dyes or additives, the current technology can be employed to offer superior coloring with outstanding colorfastness.

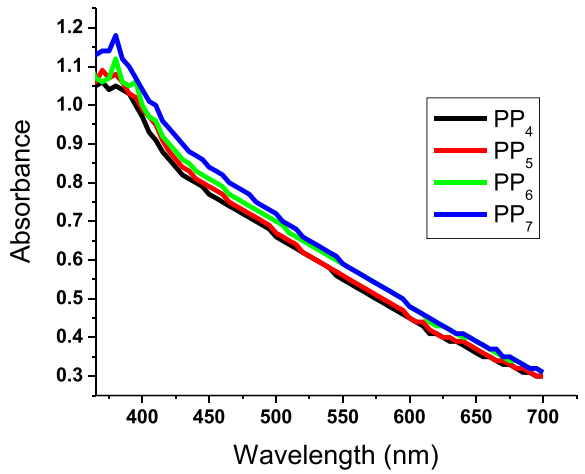

Fig. 7 Absorbance spectra of polypropylene textiles (Color figure online)

4 Conclusion

To immobilize a composite of AgNPs, PANi, and TMHDS into polypropylene textiles, we adopted a simple and cheap in situ pad-dry-cure approach. We created multifunctional technical polypropylene fibers that are hydrophobic, antimicrobial, UV-protective, and electroconductive. PANi and AgNPs were synthesized in situ using $AgNO_3$ as oxidizing agent and aniline as reducing agent, and immobilized into plasma-cured polypropylene fabric. The plasma-cured AgNPs-immobilized textiles had improved visible-light absorption, electroconductivity, UV protection, hydrophobicity, and antibacterial activity compared to the uncured polypropylene. As a result of being deposited, AgNPs (5–18 nm) have improved UV blocking and antibacterial capabilities. PANi deposition is responsible for the increased electrical conductivity, while TMHDS deposition is responsible for the enhanced water-repellency. Microwave heating was employed to cure the polypropylene fabrics after deposition of TMHDS. These features were achieved without sacrificing the mechanical properties of polypropylene. SEM and EDX analyses verified the presence of Ag^0 NPs on fabrics. The electroconductivity of the AgNPs/PANi composite on the polypropylene samples was enhanced by the incorporation of AgNPs into the AgNPs/PANi nanocomposite. Nanocomposite of AgNPs/PANi/TMHDS deposited onto plasma-treated polypropylene resulted in an electrical conductivity of 0.7618 S cm^{-1}. The PANi/AgNPs nanocomposite significantly improved antibacterial efficacy against *E. coli* and *S. aureus* compared to PANi-finished fabric. The blank polypropylene exhibited no antibacterial action. The AgNPs/PANi/TMHDS nanocomposite, when incorporated into plasma-cured polypropylene, exhibited a superhydrophobic characteristic with a contact angle of up to 153.6°. It was determined by analyzing CIE Lab parameters, color strength and UV–Vis absorbance spectra how AgNPs affected the coloration of polypropylene fibers. A strong absorbance band at 379 nm was observed for untreated PP_4 and PP_6 textiles, suggesting a pink color, but a stronger absorption band at 379 nm was observed in treated PP_5 and PP_7 fabrics,

Table 5 Colorfastness screening of polypropylene textiles

Sample	Washing		Rubbing		Perspiration				Light
	Alt.	Alt.	Dry	Wet	Acid		Alkali		
					Alt.	St.	Alt.	St.	
PP_4	3	3	2–3	2–3	3	3	3	3	4
PP_5	4–5	4–5	4–5	4	4	4–5	4–5	4–5	6
PP_6	3–4	3–4	3	3	3–4	3–4	3–4	3–4	4–5
PP_7	4–5	4–5	4–5	4	4	4–5	4–5	4–5	6

Alt is alteration of color; St is staining to cotton.

indicating a dark blue color. Measurements of air-permeability and stiffness confirmed high level of comfort. This simple technique prepares and in situ incorporates PANi and AgNPs into plasma-cured nonwoven polypropylene textiles, resulting in useful multi-function polypropylene with potential medical applications including protective coatings, wound treatment, and wearable electronics.

Acknowledgement The authors extend their appreciation to the Deputyship for Research& Innovation, "Ministry of Education" in Saudi Arabia for funding this research work through the project number (IFKSUDR_P111).

Author Contributions All authors contributed to the study conception and design, material preparation, data collection and analysis. All authors wrote the manuscript read and approved the final manuscript. All authors performed the experimental and discussed the obtained data, wrote the main manuscript text and prepared the figures. All authors reviewed the manuscript.

Data Availability All relevant data are within the manuscript and available from the corresponding author upon request.

Declarations

Competing interests The authors have no relevant financial or non-financial interests to disclose.

Ethical Approval Not applicable.

Consent to Participate Not applicable.

Consent for publication Not applicable.

References

1. I.S. Tania, M. Ali, M. Azam, J. Inorg. Organomet. Polym. Mater. **31**, 4065 (2021)
2. A.M. Elbarbary, M.A. Elhady, Y.H. Gad, J. Inorg. Organomet. Polym. Mater. **32**, 4039 (2022)
3. S.N. Aboutorabi, M. Nasiriboroumand, P. Mohammadi, H. Sheibani, H. Barani, J. Inorg. Organomet. Polym. Mater. **28**, 2525 (2018)
4. M.F. Favatela, J. Otarola, V.B. Ayala-Peña, G. Dolcini, S. Perez, A.T. Nicolini, V.A. Alvarez, V.L. Lassalle, J. Inorg. Organomet. Polym. Mater. **32**, 1473 (2022)
5. M. Asadi, M. Montazer, J. Inorg. Organomet. Polym. Mater. **23**, 1358 (2013)
6. J. Jin, Q. Dong, Z. Shu, W. Wang, K. He, Procedia Eng. **71**, 304 (2014)
7. O. Faruk, A.K. Bledzki, H. Fink, M. Sain, Macromol. Mater. Eng. **299**, 9 (2014)
8. M.D. Albaqami, S.F. Shaikh, A. Nafady, Mater. Chem. Phys. 125133 (2021)
9. J. Lieb, Med. Hypotheses **69**, 8 (2007)
10. Z. Xiong, L. Wenbin, H. Qian, T. Lei, X. He, Y. Hu, P. Lei, Front. Mater. **8**, 10 (2021)
11. S.Y. Jeong, S.-K. Park, Y.C. Kang, J.S. Cho, Chem. Eng. J **351**, 559 (2018)
12. M. Tata, V.T. John, Y.Y. Waguespack, G.L. McPherson, J. Am. Chem. Soc. **116**, 9464 (1994)
13. G. Chen, Y. Li, M. Bick, J. Chen, Chem. Rev. **120**, 3668 (2020)
14. M.C. Biswas, S. Chakraborty, A. Bhattacharjee, Z. Mohammed, Adv. Funct. Mater. **31**, 2100257 (2021)
15. C. Paquot, IUPAC, *Standard Methods for the Analysis of Oils, Fat and Derivatives*, 7th edn. (Blackwell Scientific, London, 1987)
16. J. Qu, P. Huang, L. Zhang, Y. Qiu, H. Qi, A. Leng, D. Shang, Int. J. Biol. Macromol. **161**, 24 (2020)
17. J. Choi, O.-C. Kwon, W. Jo, H.J. Lee, M.-W. Moon, 3D Print. Addit. Manuf. **2**, 159 (2015)
18. I.N. Qureshi, A. Tahira, K. Aljadoa, A.M. Alsalme, A.A. Alothman, A. Nafady, A. Karsy, Z.H. Ibupoto, J. Mater. Sci. Mater. Electron. **32**, 15594 (2021)
19. H. Zare, S. Nayebzadeh, A. Davodiroknabadi, S.H. Hataminasab, Autex Res. J. **21**, 403 (2021)
20. R. Memon, A.A. Memon, A. Nafady, S.T.H. Sherazi, A. Balouch, K. Memon, N.A. Brohi, A. Najeeb, Int. Nano Lett. **11**, 263 (2021)
21. T. Shaikh, A. Nafady, F.N. Talpur, M.H. Sirajuddin, M.R. Agheem, S.T.H. Shah, R.A. Sherazi, Soomro, S. Siddiqui, Sens. Actuators B Chem. **211**, 359 (2015)
22. K.M.M. Kabir, Y.M. Sabri, A.E. Kandjani, G.I. Matthews, M. Field, L.A. Jones, A. Nafady, S.J. Ippolito, S.K. Bhargava, Langmuir **31**, 8519 (2015)
23. L. Liao, P. Zhang, Processes **6**, 125 (2018)
24. D. Raafat, H. Sahl, Microb. Biotechnol. **2**, 186 (2009)
25. C. Bavatharani, E. Muthusankar, S.M. Wabaidur, Z.A. Alothman, K.M. Alsheetan, M. Mana AL-Anazy, D. Ragupathy, Synth. Met. **271**, 116609 (2021)
26. S. Bhagat, A.K. Chakraborti, J. Org. Chem. **72**, 1263 (2007)
27. V.K. Sharma, R.A. Yngard, Y. Lin, Adv. Colloid Interface Sci. **145**, 83 (2009)
28. H.M. Abumelha, A. Hameed, K.M. Alkhamis, J. Alkabli, E. Aljuhani, R. Shah, N.M. El-Metwaly, ACS Omega **6**, 27315 (2021)
29. A.A. Menazea, J. Mol. Struct. **1207**, 127807 (2020)
30. M. Naebe, Q. Li, A. Onur, R. Denning, Cellulose **23**, 2129 (2016)
31. Y. Lin, H. Li, Q. Wang, Z. Gong, J. Tao, Appl. Surf. Sci. **507**, 145062 (2020)
32. A.M. Ribeiro, T.H.S. Flores-Sahagun, R.C. Paredes, J. Mater. Sci. **51**, 2806 (2016)
33. M. Gao, B.Z. Tang, ACS Sens. **2**, 1382 (2017)
34. J. Shi, X. Sun, S. Zheng, X. Fu, Y. Yang, J. Wang, H. Zhang, Adv. Opt. Mater. **7**, 1900526 (2019)
35. R. Iqbal, Z. Mehmood, A. Baig, N. Khalid, Food Bioprod. Process **123**, 304 (2020)
36. F.S.A. Khan, N.M. Mubarak, M. Khalid, R. Walvekar, E.C. Abdullah, A. Ahmad, R.R. Karri, H. Pakalapati, Sci. Rep. **11**, 1 (2021)
37. Z. Abdeen, S.G. Mohammad, M.S. Mahmoud, Environ. Nanotechnol. Monit. Manag. **3**, 1 (2015)
38. T. Tiainen, M. Lobanova, E. Karjalainen, H. Tenhu, S. Hietala, Polymers (Basel) **12**, 507 (2020)
39. F. Sahin, N. Celik, A. Ceylan, S. Pekdemir, M. Ruzi, M.S. Onses, Chem. Eng. J. **431**, 133445 (2022)
40. X. Lan, B. Zhang, J. Wang, X. Fan, J. Zhang, Colloids Surf. A Physicochem. Eng. Asp. **624**, 126820 (2021)
41. N. Celik, I. Torun, M. Ruzi, M.S. Onses, J. Appl. Polym. Sci. **138**, 51358 (2021)
42. N. Celik, S. Altındal, Z. Gozutok, M. Ruzi, M.S. Onses, J. Coat. Technol. Res. **17**, 785 (2020)
43. Y.-N. Gao, Y. Wang, T.-N. Yue, Y.-X. Weng, M. Wang, J. Colloid Interface Sci. **582**, 112 (2021)
44. A. Hameed, E. Aljuhani, T.M. Bawazeer, S.J. Almehmadi, A.A. Alfi, H.M. Abumelha, G.A.M. Mersal, N. El-Metwaly, Luminescence **36**, 1781 (2021)
45. J. Ou, F. Wang, W. Li, M. Yan, A. Amirfazli, Prog. Org. Coat. **146**, 105700 (2020)

46. J. Zimmermann, S. Seeger, F.A. Reifler, Text. Res. J. **79**, 1565 (2009)
47. T.A. Singh, J. Das, P.C. Sil, Adv. Colloid Interface Sci. **286**, 102317 (2020)
48. P. Naderi, M. Zarei, S. Karbasi, H. Salehi, Eur. Polym. J. **124**, 109502 (2020)
49. D. Zhou, J. Chen, B. Liu, X. Zhang, X. Li, T. Xu, Bioprinting **16**, e00060 (2019)
50. N. Vigneshwaran, A. Arputharaj, *Advances in Functional Finishing of Textiles* (Springer, Singapore, 2020), pp. 43–56
51. S. Tandon, B. Kandasubramanian, S.M. Ibrahim, Ind. Eng. Chem. Res. **59**, 17593 (2020)
52. S. Khorshidi, A. Solouk, H. Mirzadeh, S. Mazinani, J.M. Lagaron, S. Sharifi, S. Ramakrishna, J. Tissue Eng. Regen. Med. **10**, 715 (2016)
53. M. Hussain, A. Nafady, S.T.H. Sherazi, M.R. Shah, A. Alsalme, M.S. Kalhoro, S.A. Mahesar, S. Siddiqui, RSC Adv. **6**, 82882 (2016)
54. W.-H. Dong, J.-X. Liu, X.-J. Mou, G.-S. Liu, X.-W. Huang, X. Yan, X. Ning, S.J. Russell, Y.-Z. Long, Colloids Surf. B Biointerfaces **188**, 110766 (2020)
55. I.R. Mary, R. Leethiyal, P. Sekar, D. Mangalaraj, C. Viswanathan, N. Ponpandian, Mater. Today Proc. **18**, 1729 (2019)
56. N. Romano, C. Zeng, Rev. Fish. Sci. **21**, 1 (2013)
57. M. Naebe, A.N.M.A. Haque, A. Haji, Engineering **12**, 145 (2021)
58. I.A. Gass, C.J. Gartshore, D.W. Lupton, B. Moubaraki, A. Nafady, A.M. Bond, J.F. Boas, J.D. Cashion, C. Milsmann, K. Wieghardt, Inorg. Chem. **50**, 3052 (2011)
59. A.I. Ribeiro, D. Senturk, K.S. Silva, M. Modic, U. Cvelbar, G. Dinescu, B. Mitu, A. Nikiforov, C. Leys, I. Kuchakova, *IOP Conference Series: Materials Science and Engineering* (IOP Publishing, Bristol, 2018), p. 12007
60. A. Akbarzadeh, M. Samiei, S. Davaran, Nanoscale Res. Lett. **7**, 144 (2012)
61. T. Varadavenkatesan, R. Selvaraj, R. Vinayagam, Mater. Today Proc. **23**, 39 (2020)
62. T.A. Skotheim, *Handbook of Conducting Polymers* (Marcel Dekker, New York, 1986)
63. T.A. Khattab, A.L. Mohamed, A.G. Hassabo, Mater. Chem. Phys. **249**, 122981 (2020)
64. M. Kankofer, G. Kolm, J. Aurich, C. Aurich, Theriogenology **63**, 1354 (2005)